Redox Biology 27 (2019) 101075

Contents lists available at ScienceDirect

Redox Biology

journal homepage: www.elsevier.com/locate/redox

Research Paper

Glucose-dependent trans-plasma membrane electron transport and p70^{S6k} phosphorylation in skeletal muscle cells

Shannon C. Kelly[1], Neej N. Patel, Amanda M. Eccardt, Jonathan S. Fisher*

Department of Biology, Saint Louis University, St. Louis, MO, United States

ARTICLE INFO

Keywords:
Glucose 6-phosphate dehydrogenase
Superoxide
Hydrogen peroxide
Glycolysis
Glucose sensing

ABSTRACT

The reduction of extracellular oxidants by intracellular electrons is known as trans-plasma membrane electron transport (tPMET). The goal of this study was to characterize a role of tPMET in the sensing of glucose as a physiological signal. tPMET from C2C12 myotubes was monitored using a cell-impermeable extracellular electron acceptor, water-soluble tetrazolium salt-1 (WST-1). Superoxide dismutase in the incubation medium or exposure to an NADPH oxidase (NOX) isoform 1/4 inhibitor suppressed WST-1 reduction by 70%, suggesting a role of NOXs in tPMET. There was a positive correlation between medium glucose concentration and WST-1 reduction, suggesting that tPMET is a glucose-sensing process. WST-1 reduction was also decreased by an inhibitor of the pentose phosphate pathway, dehydroepiandrosterone. In contrast, glycolytic inhibitors, 3PO and sodium fluoride, did not affect WST-1 reduction. Thus, it appears that glucose uptake and processing in the pentose phosphate pathway drives NOX-dependent tPMET. Western blot analysis demonstrated that p70^{S6k} phosphorylation is glucose-dependent, while the phosphorylation of AKT and MAPK did not differ in the presence or absence of glucose. Further, phosphorylation of p70^{S6k} was dependent upon NOX enzymes. Finally, glucose was required for full stimulation of p70^{S6k} by insulin, again in a fashion prevented by NOX inhibition. Taken together, the data suggest that muscle cells have a novel glucose-sensing mechanism dependent on NADPH production and NOX activity, culminating in increased p70^{S6k} phosphorylation.

1. Introduction

Trans plasma membrane electron transport (tPMET) has been implicated in physiological functions such as cell growth, iron metabolism, cell signaling, and protection of the cell from reactive oxygen species and bacteria [1–4]. tPMET has also been implicated in the pathogenesis of cardiovascular disease, cancer, neurodegenerative diseases, as well as pulmonary disease [5–9].

One of the primary examples of enzyme-mediated tPMET is catalyzed by NADPH oxidases (NOXs). These enzymes utilize intracellular NADPH to reduce extracellular oxygen to superoxide as the mode for tPMET [10]. Previous research has shown that a muscle cell line, primary mouse myotubes, and isolated skeletal muscle tissue are capable of tPMET [11]. Further, cultured muscle cells are capable of shuttle-based tPMET through the export of ascorbate, and this process is glucose-dependent [11,12]. Additionally, the addition of superoxide dismutase in the culture medium suppressed tPMET in muscle cells, suggesting that superoxide could play a role in tPMET in muscle cells [12].

Since tPMET has been hypothesized to be a universal system among living organisms and has been implicated in cell signaling, protection of cells from ROS, and disease pathogenesis, an objective of this study was to characterize glucose-dependent tPMET. We hypothesized that glucose-dependent NOX activity could alter intracellular signaling pathways. Here, we show that tPMET is a glucose-sensing process utilizing the pentose phosphate pathway and NADPH oxidases, and we demonstrate a novel NOX-dependent glucose sensing pathway leading to phosphorylation of p70^{S6k}.

2. Materials and methods

2.1. Materials

C2C12 myoblasts, a mouse muscle cell line, and L6 myoblasts, a rat muscle cell line, were obtained from American Type Culture Collection (Manassas, VA, USA). Dulbecco's modified Eagle's medium-low glucose (DMEM), phosphate buffered saline (PBS), penicillin-streptomycin, trypsin-EDTA, phenazine methosulfate (PMS), D-glucose, pyruvate, superoxide dismutase (SOD), 2-deoxy-D-glucose (2DG),

* Corresponding author.
E-mail address: jonathan.fisher@slu.edu (J.S. Fisher).
[1] Current address: Department of Biomedical Sciences, University of Missouri, Columbia, MO, United States.

https://doi.org/10.1016/j.redox.2018.101075
Received 1 November 2018; Received in revised form 7 December 2018; Accepted 10 December 2018
Available online 12 December 2018

dehydroepiandrosterone (DHEA), (2E)-3-(3-pyridinyl)-1-(4-pyridinyl)-2-propen-1-one (3PO), 1,2-bis(2-aminophenoxy)ethane-N,N,N′,N′-tetraacetic acid tetrakis (acetoxymethyl ester) (BAPTA-AM), diphenyleneiodonium (DPI), N,N′-dimethylthiourea (DMTU), 4-hydroxy-TEMPO (Tempol), and glucose oxidase were purchased from Sigma Aldrich (St. Louis, MO, USA). FetalPlex animal serum complex was purchased from Gemini Bio-Products (Woodland, CA, USA). Horse serum was purchased from Gibco Technologies (Gaithersburg, MD, USA). 2-(4-iodophenyl)-3-(4-nitrophenyl)-5-(2,4-disulfophenyl)-2H-tetrazolium sodium salt (WST-1) was purchased from Accela ChemBio Inc (San Diego, CA, USA). GKT137831 was purchased from Selleck Chemicals (Houston, TX, USA). GSK2795039 was purchased from ChemScene (Monmouth Junction, NJ, USA). Mn(III)tetrakis(4-benzoic acid)porphyrin chloride (MnTBAP) was purchased from EMD Biosciences, Inc (San Diego, CA, USA). Primary antibodies against phospho-AKT (Ser473), phospho-AKT (Thr308), AKT, phospho-p70 S6K, p70 S6K, phospho-p38, p38, phospho-p42/44, and GAPDH (conjugated to horseradish peroxidase [HRP]) were obtained from Cell Signaling Technologies, Inc (Danvers, MA, USA). NOX1 primary antibody was purchased from Invitrogen (Carlsbad, CA, USA). NOX2 primary antibody was purchased from Sigma Aldrich (St. Louis, MO, USA). NOX4 primary antibody was purchased from Millipore (Burlington, MA, USA). HRP-conjugated goat-anti-rabbit and goat-anti-mouse secondary antibodies were obtained from Thermo Scientific (Rockford, IL, USA). Nitroblue tetrazolium salt (NBT) was purchased from Thermo Fisher Scientific (Rockford, IL, USA). Calcium green-1AM was purchased from Invitrogen (Carlsbad, CA, USA).

2.2. Animals

Male C57 Black 6 mice were purchased from Jackson Laboratory (Bar Harbor, ME, USA). The mice were housed in a temperature-controlled environment with a 12-h light-dark cycle as well as food and water freely available. Mice were anesthetized using pentobarbital (50 mg/kg, IP), and brain, heart, kidney, liver, tibialis anterior (TA), soleus (SOL), and extensor digitorum longus (EDL) were harvested and frozen with clamps cooled in liquid nitrogen for use in NOX expression and activity. Procedures using live animals were approved by the Saint Louis University Institutional Animal Care and Use Committee (IACUC approval number 2453).

2.3. Cell culture

C2C12 myoblasts were cultured in Dulbecco's modified Eagle's medium (DMEM) supplemented with 10% FetalPlex and 1% penicillin-streptomycin at 37 °C with 5% CO_2 [11]. Myoblasts were seeded into 12-well plates or the first six rows of 96-well plates. Once 90% confluence was reached, the myoblasts were differentiated to myotubes with DMEM supplemented with 2% horse serum and 1% penicillin-streptomycin. The same procedure was utilized to culture L6 myoblasts, except they were seeded in 6-well plates before differentiation.

2.4. WST-1 assay

The WST-1 reduction protocol follows the methods presented by Kelly et al. [12]. Briefly, 96-well plates with myotubes in the first six rows were washed with PBS. An assay solution containing 5 mM glucose, 400 μM WST-1, and 20 μM PMS in HEPES buffered saline (HBS: 20 mM HEPES sodium salt, 140 mM sodium chloride, 5 mM potassium chloride, 2.5 mM magnesium sulfate, and 1 mM calcium chloride) [13] was added to the entire plate, as the last two rows without cells were used to monitor any background reaction. Absorbance was monitored every ten minutes for one hour at 438 nm in a Powerwave X-1 spectrophotometric plate reader (BioTek, Winooski, VT, USA). Then, the myotubes were washed with PBS, and a bicinchoninic acid (BCA) protein assay was performed with bovine serum albumin standards (Thermo Scientific, Rockford, IL, USA).

To determine the fraction of WST-1 reduction that was attributable to various metabolic pathways, enzymes or inhibitors were added to the WST-1 solution. For example, to assess the contribution of superoxide to tPMET, SOD was added to the WST-1 solution in concentrations ranging from 0 kU/mL to 250 kU/mL. Another assay included 5 mM 2DG to determine whether hexokinase supports tPMET. When monitoring other metabolic contributors to tPMET, cells were pretreated in differentiation media supplemented with GKT137831 (0–100 μM), GSK2795039 (0–100 μM), DHEA (200 μM), 3PO (10 μM), or sodium fluoride (2 mM) for one hour. The WST-1 assay was performed in the presence or absence of the inhibitor. When glucose-dependence was monitored, 2 mM pyruvate was used in lieu of glucose during the WST-1 reduction assay.

2.5. Effects of glucose

C2C12 myotubes were washed with PBS and pretreated in HBS supplemented with either 2 mM sodium pyruvate or 5 mM glucose at 37 °C with 5% CO_2. On ice, the cells were washed with PBS twice and harvested with lysis buffer (50 mM HEPES pH 7.4, 150 mM sodium chloride, 10% glycerol, 1% Triton X-100, 1.5 mM magnesium chloride, 1 mM EDTA, 10 mM sodium pyrophosphate, 100 mM sodium fluoride, 2 mM sodium orthovanadate, 10 μg/mL aprotinin, 10 μg/mL leupeptin, 0.5 μg/mL pepstatin, and 0.2 mM phenylmethylsulfonyl fluoride) [14]. Lysates were centrifuged for 10 min at 12,000 rpm at 4 °C. The pellet was discarded, and the protein in the supernatant was quantified with a BCA protein assay and prepared in Laemmli sample buffer containing dithiothreitol for western blot analysis. When monitoring the effect of enzymes or inhibitors, cells were treated with 60 kU/mL SOD, 100 kU/mL catalase, or 20 μM DPI in addition to 2 mM pyruvate or 5 mM glucose. Cells were pretreated with 100 μM MnTBAP, 5 mM DMTU, or 1 mM Tempol for 1 h in differentiation media at 37 °C prior to treatment of cells with 2 mM pyruvate or 5 mM glucose in HBS. To determine the effect of the presence or absence of glucose on insulin signaling, cells were incubated for one hour in medium containing either glucose or pyruvate and then exposed to 5 nM insulin for 20 min. When monitoring the effect of extracellular peroxide on intracellular signaling, cells were treated in HBS supplemented with 5 mM glucose in the presence or absence of 50 mU/mL glucose oxidase, which generates hydrogen peroxide, for 15 min.

2.6. Western blot

Frozen mouse tissue sample was homogenized in lysis buffer (50 mM HEPES pH 7.4, 150 mM sodium chloride, 10% glycerol, 1.5 mM magnesium chloride, 1 mM EDTA, 10 mM sodium pyrophosphate, 100 mM sodium fluoride, 2 mM sodium orthovanadate, 10 μg/mL aprotinin, 10 μg/mL leupeptin, 0.5 μg/mL pepstatin, and 0.2 mM phenylmethylsulfonyl fluoride) [11] with 0.5 mm zirconium oxide beads (Midwest Scientific, St. Louis, MO, USA) in a bullet blender (Next Advance, Averill Park, NY, USA). After homogenization, 1% Triton X-100 (final concentration) was added to the tissue samples. C2C12 and L6 myoblasts were harvested on ice in lysis buffer with 1% Triton X-100. Protein of tissue and whole cell homogenate was then quantified using BCA protein assay. Samples were prepared in Laemmli sample buffer plus dithiothreitol, except that samples analyzed for NOX4 were prepared in Laemmli sample buffer without dithiothreitol. Samples were run on 4–20% polyacrylamide SDS gels from Bio-Rad (Hercules, CA, USA), Expedeon Inc RunBlue (San Diego, CA, USA), and GenScript (Piscataway, NJ, USA). Invitrogen 3–8% Tris-Acetate gels were utilized to analyze NOX1 and NOX2 protein. Protein was then transferred to nitrocellulose membranes (Thermo Scientific, Rockford, IL, USA). For native gel electrophoresis, homogenized mouse tissue and whole cell lysate were prepared with 2x native sample buffer (62.5 mM Tris-HCl pH 6.8, 40% glycerol, 0.01% bromophenol blue) [15] and run on 7.5%

resolving and 4% stacking native gels. The gels were incubated in 2% SDS for 1 h prior to transfer. Membranes were blocked in 5% milk in Tris-buffered saline with 0.1% Tween (TBST). Membranes were then incubated with primary antibody, followed by secondary antibody and imaged using chemiluminescence (Midwest Scientific, St. Louis, MO, USA). Membranes were quantified using ImageJ software (National Institute of Health, Bethesda, MA, USA).

2.7. Native gel NADPH oxidase activity assay

Homogenized mouse tissue and whole cell lysate were prepared with 2x native sample buffer, as described above, and were run on 7.5% resolving and 4% stacking native gels. Gels were then incubated in NBT solution (50 mM Tris-HCl, pH7.4, 100 μM magnesium chloride, 1 mM calcium chloride, and 0.2 mM NBT) [16] for 20 min protected from light. After 20 min, 200 μM NADPH was added, and the gels were incubated for one hour protected from light, or until blue precipitate bands formed. The addition of 50 μM GKT137831 or 20 μM GSK2795039 was utilized to monitor roles of specific isoforms of NOX enzymes. The gels were washed in diH_2O three times after the formation of precipitate bands and imaged using ThermoFisher Scientific iBright FL1000.

2.8. Calcium green assay

In a 96-well plate of C2C12 myotubes, cells were washed with PBS. The cells were then pretreated for 30 min at 37 °C in PBS supplemented with 5 mM glucose and 4 μM calcium green-1AM, and some cells were also incubated with 30 μM BAPTA-AM [13,17] as a negative control. Cells were then washed in PBS and incubated in HBS supplemented with 5 mM glucose or 2 mM pyruvate as well as in the presence or absence of 60 U/mL SOD. Calcium green-1AM fluorescence was monitored for one hour in a BioTek FLx800 microplate fluorescence reader with an excitation of 485 nm and emission of 528 nm.

2.9. Statistical analysis

Statistical analysis was performed with Rstudio software (Boston, MA, USA). An ANOVA with repeated measures was utilized to analyze WST-1 assays, and ANOVA was employed to analyze western blots with Tukey Honest Significant Difference (HSD) post hoc tests (α-level = 0.05).

3. Results

3.1. tPMET in C2C12 myotubes

To assess the role of superoxide in tPMET, we utilized SOD, which catalyzes the partitioning of superoxide into oxygen or hydrogen peroxide. As shown in Fig. 1, C2C12 myotubes were able to reduce WST-1 in the absence of SOD, indicating that the myotubes are capable of transporting electrons to the extracellular media. Upon addition of SOD to the extracellular media, WST-1 reduction was significantly decreased, indicating that superoxide production is the primary mechanism of tPMET in C2C12 myotubes. There appears to be a dose dependent decrease of WST-1 reduction in the presence of SOD that was nearly maximal with 60 U/mL SOD. Therefore, the concentration of 60 U/mL was used in subsequent procedures.

In C2C12 myotubes, it was previously reported that NOX isoforms 1, 2, and 4 are expressed [18]. When the NOX1/4 inhibitor GKT137831 was added to the extracellular media, there was a significant suppression of WST-1 reduction, with the maximum reduction around 50 μM (Fig. 2A). When NOX2 inhibitor GSK2795039 was added to the extracellular media, there was no suppression of WST-1 reduction up to 100 μM (Fig. 2B). This indicates that NOX isoform 1 or 4 is responsible for the production of electrons that reduce WST-1 and not NOX isoform

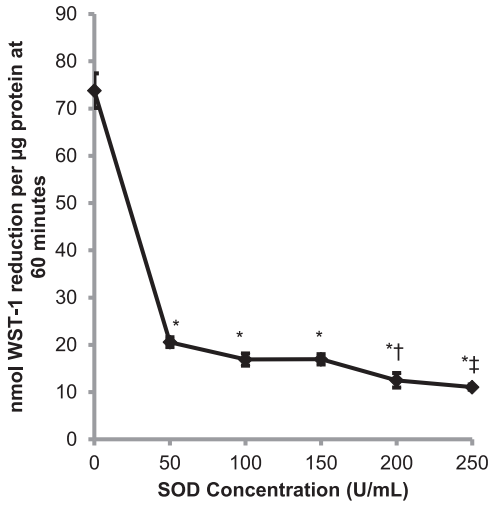

Fig. 1. Superoxide dismutase suppressed the reduction of WST-1. tPMET was monitored using 400 μM WST-1 and 20 μM PMS in HBS supplemented with 5 mM glucose. SOD (0–250 U/mL) was added to the extracellular media, and absorbance was monitored for 60 min (N = 12/group). Error bars represent standard error of the mean. ANOVA with repeated measures was performed *p < 0.05 vs 0 U/mL, †p < 0.05 vs 50 U/mL, ‡p < 0.05 vs 50, 100, and 150 U/mL.

2. To verify the WST-1 reduction results, a native gel NADPH oxidase activity assay was performed. This assay detects superoxide by its reduction of NBT to a blue precipitate. In the presence of NADPH and without the addition of an inhibitor, NBT was reduced by all tissue and cell samples (Figs. 2C, 2D). In the presence of GKT137831 there was suppression of NBT precipitate formation in all tissue samples (Fig. 2C). In the presence of GSK2795039, though, there was no inhibition of the formation of NBT precipitate (Fig. 2D). This further verifies that either NOX1 or NOX4 is involved in the production of superoxide in C2C12 myotubes.

Since the IC_{50} of GKT137831 toward NOX1 and NOX4 is similar (0.14 μM for NOX1 and 0.11 μM for NOX4) [19], we could not establish which isoform is involved in the mechanism of tPMET by means of a dose-response curve. Thus, we assessed which NOX isoforms are present in muscle cells. As shown in Fig. 3, NOX1 and NOX2 proteins were present in C2C12 myotubes, while NOX4 protein was absent. The presence of NOX1 but not NOX4 was further verified by western blot analysis after native gel electrophoresis (Fig. 3C). In conjunction with the WST-1 assays and native gel activity assays (Fig. 2), the data show that NOX1 is the primary source of reactive oxygen species for this mechanism of tPMET in C2C12 myotubes.

Previous data in our lab has shown that tPMET is dependent upon facilitative glucose transporter 1 (GLUT1) and not GLUT4 [11]. To further understand the role of glucose in the mechanism of tPMET, we looked at reduction of WST-1 by cells incubated with various concentrations of glucose. As shown in Figs. 4A and 4B, reduction of WST-1 by C2C12 myotubes is almost completely suppressed by the absence of glucose. Thus, although there are multiple mechanisms for tPMET [10], the majority of tPMET under basal conditions in myotubes appears to be glucose-dependent. As shown by the scatterplot inset of Fig. 4A, there was a statistically significant positive correlation between WST-1 reduction and 1–5 mM glucose ($r = 0.3$, $p = 0.04$). The addition of glucose after preincubation in glucose-free medium (with 2 mM pyruvate) could rescue this suppression of WST-1 reduction (Fig. 4C). When pyruvate and glucose were both present in the reaction solution, there was an increase in WST-1 reduction compared to glucose alone (Fig. 4D). This could suggest that in the presence of pyruvate, glucose is entering the pentose phosphate pathway (PPP) rather than glycolysis.

Whether glucose enters the PPP or glycolysis, glucose is first

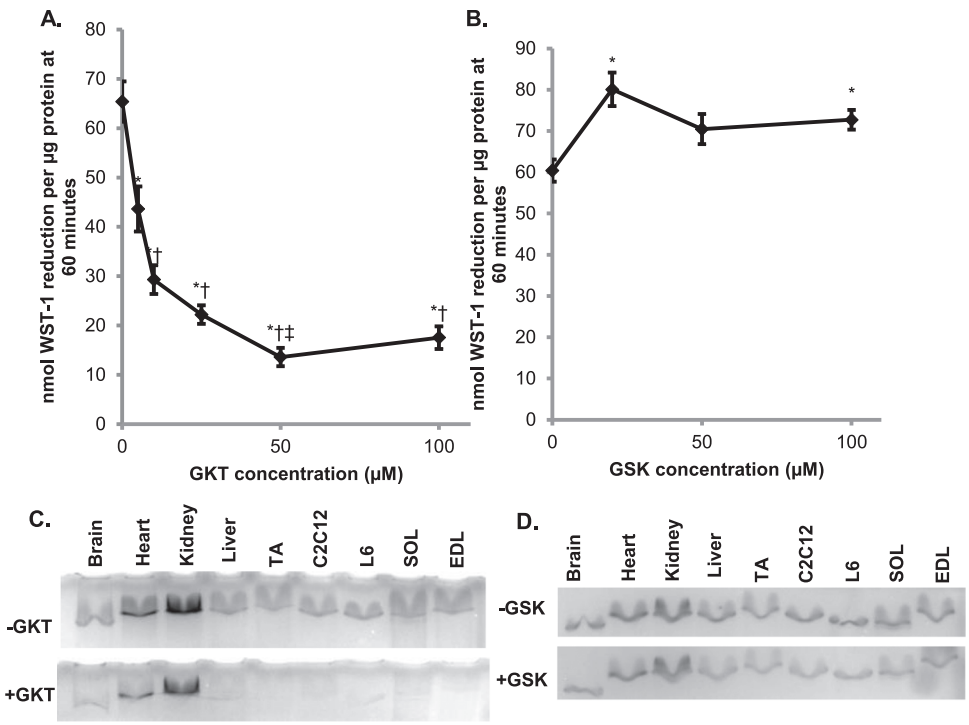

Fig. 2. A NOX1/4 inhibitor suppresses the tPMET and superoxide production A. NOX1/4 inhibitor GKT137831 (GKT) was added to the extracellular media containing 400 µM WST-1, 20 µM PMS and 5 mM glucose in HBS, and absorbance was monitored for 60 min (N = 12/group). Error bars represent standard error of the mean. ANOVA with repeated measures was performed *p < 0.05 vs 0 µM, †p < 0.05 vs 5 µM, ‡p < 0.05 vs 10 µM. **B.** NOX2 inhibitor GSK2795039 (GSK) was added to the WST-1 reaction media, and absorbance was monitored for 60 min (N = 18/group). Error bars represent standard error of the mean. ANOVA with repeated measures was performed *p < 0.05 vs 0 µM. **C.** NADPH oxidase activity in native polyacrylamide gels was monitored by reduction of NBT in the presence or absence of 50 µM GKT. **D.** NADPH oxidase activity in the presence or absence of 20 µM GSK. C2C12 = mouse muscle cell line, L6 = rat muscle cell line, TA = Tibialis anterior, SOL = Soleus, EDL = Extensor digitorum longus.

phosphorylated by hexokinase after it is taken up into the cell. In the presence of 2DG, an allosteric inhibitor of hexokinase via its intracellular accumulation as 2DG-6-phosphate, WST-1 reduction was significantly suppressed to levels similar to WST-1 reduction by cells incubated with pyruvate instead of glucose (Fig. 5). This suggests that hexokinase and the phosphorylation of glucose are involved in the mechanism of tPMET.

To further explore whether the PPP or glycolysis is involved in the mechanism of tPMET, we utilized DHEA, which inhibits glucose 6-phosphate dehydrogenase (G6PD) of the PPP [20] and two glycolytic inhibitors: 3PO which inhibits phosphofructokinase, the third step in glycolysis, and sodium fluoride which inhibits enolase, the ninth step of glycolysis [21]. Upon the addition of DHEA, WST-1 reduction was significantly suppressed, but when the glycolytic inhibitors were added, there was no significant impact on WST-1 reduction (Fig. 6A and B). This indicates that the PPP, rather than glycolysis, is involved in the process of tPMET in C2C12 myotubes.

Taken together, the data suggest a model in which glucose enters C2C12 myotubes through GLUT1 and is phosphorylated by hexokinase to G6P, after which G6P enters the PPP with resultant NADPH production. Electrons from NADPH are then used by NOX1 enzymes to produce superoxide as the main mechanism of tPMET.

3.2. Determining a functional role of tPMET in C2C12 myotubes

Previous literature has shown that superoxide and reactive oxygen species can play a role in signal transduction. We next sought to determine a functional role of tPMET and determine if the production of ROS plays a role in cell signaling. First, the role of tPMET in insulin signaling was explored through western blot analysis. In the absence of glucose, there was no significant difference in phosphorylated-AKT levels compared to the presence of glucose. This indicates that superoxide produced by tPMET in the presence of glucose does not activate insulin signaling (Fig. 7A).

Additional literature has shown that ROS can activate the MAPK pathway, specifically the p42/44MAPK (ERK1/2) pathway and the p38 MAPK pathway [22]. Western blot analysis determined that phosphorylation of p42/44 and p38 protein was not affected by the presence or absence of glucose (Fig. 7B). This suggests the activation of the MAPK pathway is not glucose sensitive. It has also been suggested that

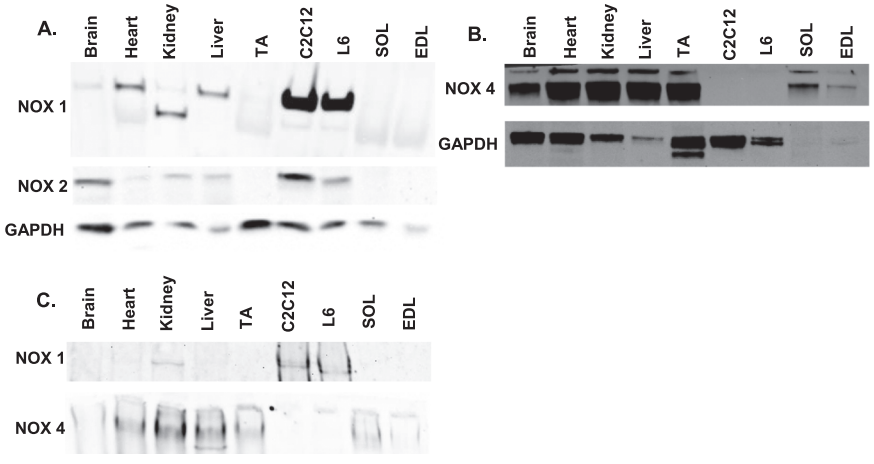

Fig. 3. C2C12 myotubes contain NOX1 and NOX2, but not NOX4 protein. A. Western blot of NOX1 and NOX2 isoforms in C2C12 myotubes. Brain, heart, kidney, liver, tibialis anterior (TA), rat muscle cell line (L6), soleus (SOL), and extensor digitorum longus (EDL) **B.** Western blot analysis of NOX4 isoform. **C.** Western blot analysis to determine the presence of NOX1 and NOX4 after native gel electrophoresis.

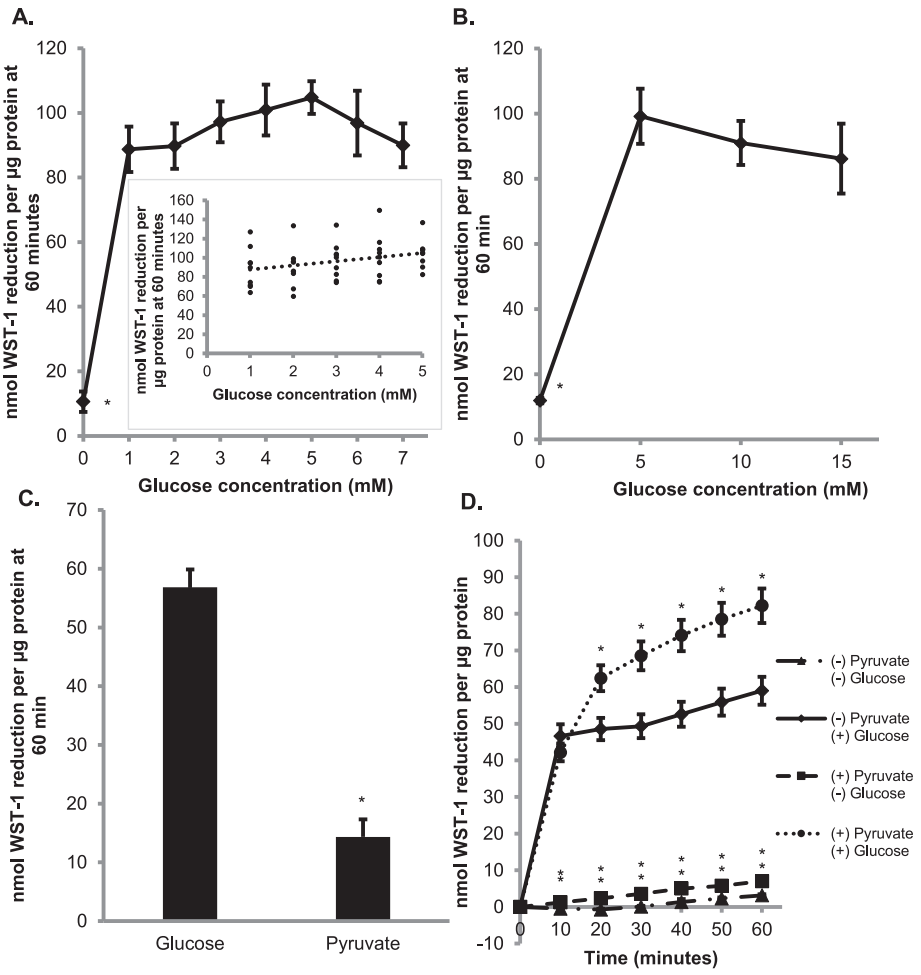

Fig. 4. tPMET is a glucose-sensitive process. **A.** 0–7 mM glucose was added to the WST-1 reaction media. 2 mM pyruvate was added in the absence of glucose. WST-1 reduction was monitored for 60 min (N = 9/group). Error bars represent standard error of the mean. ANOVA with repeated measures was performed *p < 0.05 vs 5 mM glucose. Correlation analysis is shown by the scatterplot inset (r = 0.3, p = 0.041) **B.** Similar to A, except glucose concentrations varied from 0 to 15 mM (N = 9/group). Error bars represent standard error of the mean. ANOVA with repeated measures was performed *p < 0.05 vs 5 mM glucose **C.** Myotubes were pretreated with 2 mM pyruvate. WST-1 reaction media containing either 5 mM glucose or 2 mM pyruvate was added and the absorbance was monitored for 60 min (N = 36/group). Error bars represent standard error of the mean. ANOVA was performed *p < 0.05. **D.** Myotubes were pretreated with ± pyruvate and ± glucose prior to the addition of WST-1 reaction media containing the same conditions. WST-1 reduction was monitored for 60 min (N = 18/group). Error bars represent standard error of the mean. ANOVA with repeated measures was performed *p < 0.05 vs 5 mM glucose at specific time point.

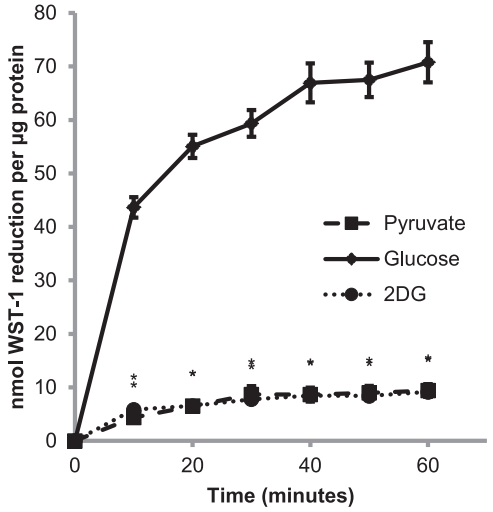

Fig. 5. 2-deoxy-D-glucose suppresses WST-1 tPMET. WST-1 reaction media was supplemented with 5 mM 2-deoxy-D-glucose (2DG), 5 mM glucose, or 2 mM pyruvate and absorbance was monitored for 60 min (N = 24/group). Error bars represent standard error of the mean. ANOVA with repeated measures was performed *p < 0.05 vs 5 mM glucose at specific time point.

ROS can activate calcium channels [23]. In the presence or absence of glucose, as well as SOD, there was no significant change in calcium green fluorescence, indicating that superoxide-mediated tPMET does not activate calcium channels (Fig. 7C).

Because reactive oxygen species have been shown to activate the $p70^{S6k}$ pathway [24], we next determined if glucose increased the phosphorylation of $p70^{S6k}$. There was a significant increase in the phosphorylation of $p70^{S6k}$ with 5 mM glucose compared to 0 mM glucose (Fig. 8A). In addition, there was a positive correlation seen between increasing concentrations of glucose and increasing phosphorylation of $p70^{S6k}$ (r = 0.57, p = 0.004). Previous literature has shown that sodium pyruvate can act as a peroxide scavenger [25], raising the possibility that pyruvate could have directly interfered with effects of superoxide, by clearing peroxide after its formation from superoxide. However, when lactic acid was utilized to supplement the 0 mM glucose condition instead of pyruvate, there was still a significant suppression in phosphorylation of $p70^{S6k}$ in the absence of glucose (data not shown). We need to acknowledge a potential role of differences in osmolarity in leading to the difference in $p70^{S6k}$ phosphorylation in cells incubated in the presence of glucose (5 mM) or the absence of glucose (supplemented with 2 mM sodium pyruvate). However, against the background osmolarity of the HEPES-buffered saline, this difference in osmolarity for the glucose-containing and sodium pyruvate-containing solutions would be relatively minimal. Furthermore, $p70^{S6k}$ phosphorylation was higher for the 4 mM glucose condition than in the matched osmolarity condition of 2 mM sodium pyruvate (0 mM glucose), suggesting that osmolarity does not explain the difference in $p70^{S6k}$ phosphorylation.

We next asked whether NADPH oxidases play a role in the increase in $p70^{S6k}$ phosphorylation. Upon the addition of DPI, a NOX inhibitor, there was a significant decrease in phosphorylation of $p70^{S6k}$, suggesting that ROS released by NOX enzymes mediate intracellular signaling (Fig. 8B). To verify that H_2O_2 can activate $p70^{S6k}$, myotubes were treated with glucose oxidase, which generates H_2O_2. There was a

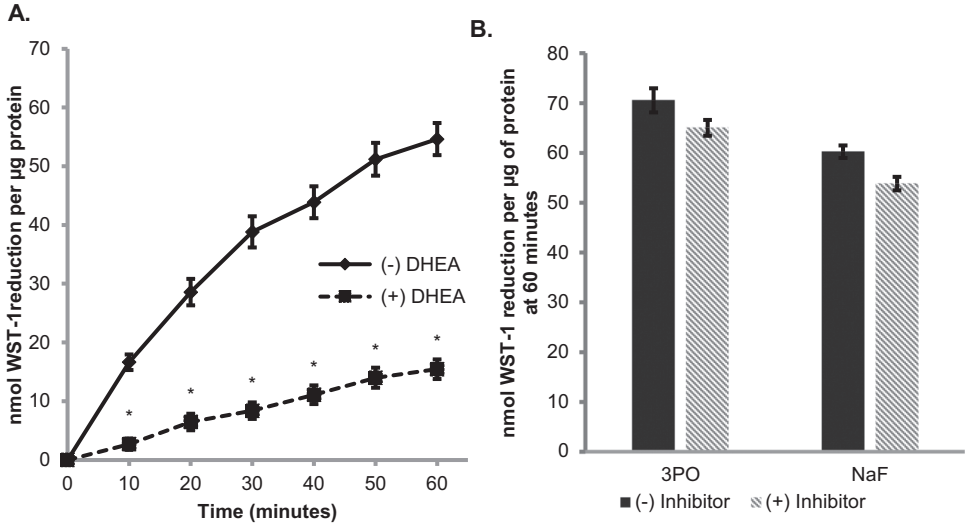

Fig. 6. tPMET relies on the pentose phosphate pathway A. Myotubes were pretreated with 200 µM DHEA for 1 h. The WST-1 assay was then performed in the presence of the inhibitor and absorbance was monitored for 60 min (N = 36/group). Error bars represent standard error of the mean. ANOVA with repeated measures was performed *p < 0.05 vs control at specific time point. **B.** WST-1 assay was performed similar to A, except 10 µM 3PO or 2 mM sodium fluoride was utilized (N = 18/group). Error bars represent standard error of the mean. ANOVA was performed *p < 0.05 vs (-) Inhibitor.

trend toward an increase in phosphorylation of $p70^{S6k}$ (p = 0.14) in cells exposed to glucose oxidase (Fig. 8C). However, upon the addition of extracellular SOD or catalase there was no suppression of phosphorylated $p70^{S6k}$ (Fig. 9A-B). This indicates that extracellular superoxide or H_2O_2 are not responsible for the phosphorylation of $p70^{S6k}$. Neither the membrane-permeable SOD mimetic MnTBAP nor the membrane-permeable radical scavenger TEMPOL affected glucose-dependent $p70^{S6k}$ phosphorylation (Fig. 9C and D), suggesting that intracellular superoxide does not play a role in this process. The membrane-permeable H_2O_2 scavenger DMTU slightly, but not statistically significantly, suppressed $p70^{S6k}$ phosphorylation (Fig. 9E). Given that extracellular H_2O_2 and superoxide did not affect $p70^{S6k}$ phosphorylation, NOX-related reduction of extracellular WST-1 may serve as a marker for organellar NOX production of ROS, leading to an increase in $p70^{S6k}$ phosphorylation potentially mediated by intracellular H_2O_2.

Given that $p70^{S6k}$ phosphorylation was responsive to glucose, we next asked whether glucose plays a role in $p70^{S6k}$ phosphorylation stimulated by insulin. In the presence of insulin, there was a significant suppression in the phosphorylation of $p70^{S6k}$ in the absence of glucose as well as a significant suppression in phosphorylation in the presence of both insulin and DPI (Fig. 10A and B). These findings suggest that $p70^{S6k}$ phosphorylation is glucose-dependent in a process involving NOX under both basal and insulin-stimulated conditions.

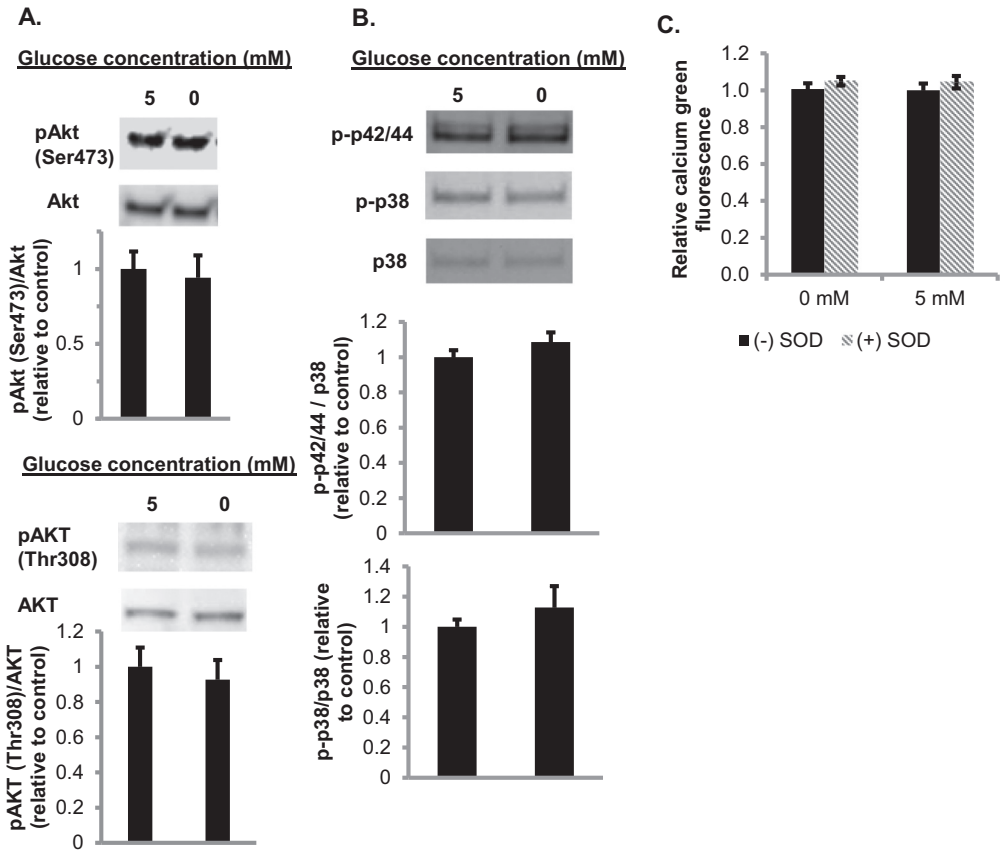

Fig. 7. AKT, the MAP kinases p38 or p42/44 (ERK1/2), and cytosolic calcium concentrations are unaffected by absence of glucose. A. Western blot analysis of the levels of phosphorylated AKT (Ser473 and Thr308) for cells incubated in the absence or presence of 5 mM glucose. Total AKT was utilized as a loading control (N = 6/group). Error bars represent standard error of the mean. ANOVA was performed. **B.** Western blot analysis of phosphorylated p38 and phosphorylated p42/44 (N = 4/group). Error bars represent standard error of the mean. ANOVA was performed. **C.** Myotubes were pretreated with 4 µM calcium green-1AM ± 30 µM BAPTA-AM. Calcium green fluorescence was assessed after 1 h in the presence or 5 mM glucose or 2 mM pyruvate and the presence or absence of 60 U/mL SOD (N = 12/group). Error bars represent standard error of the mean. ANOVA was performed.

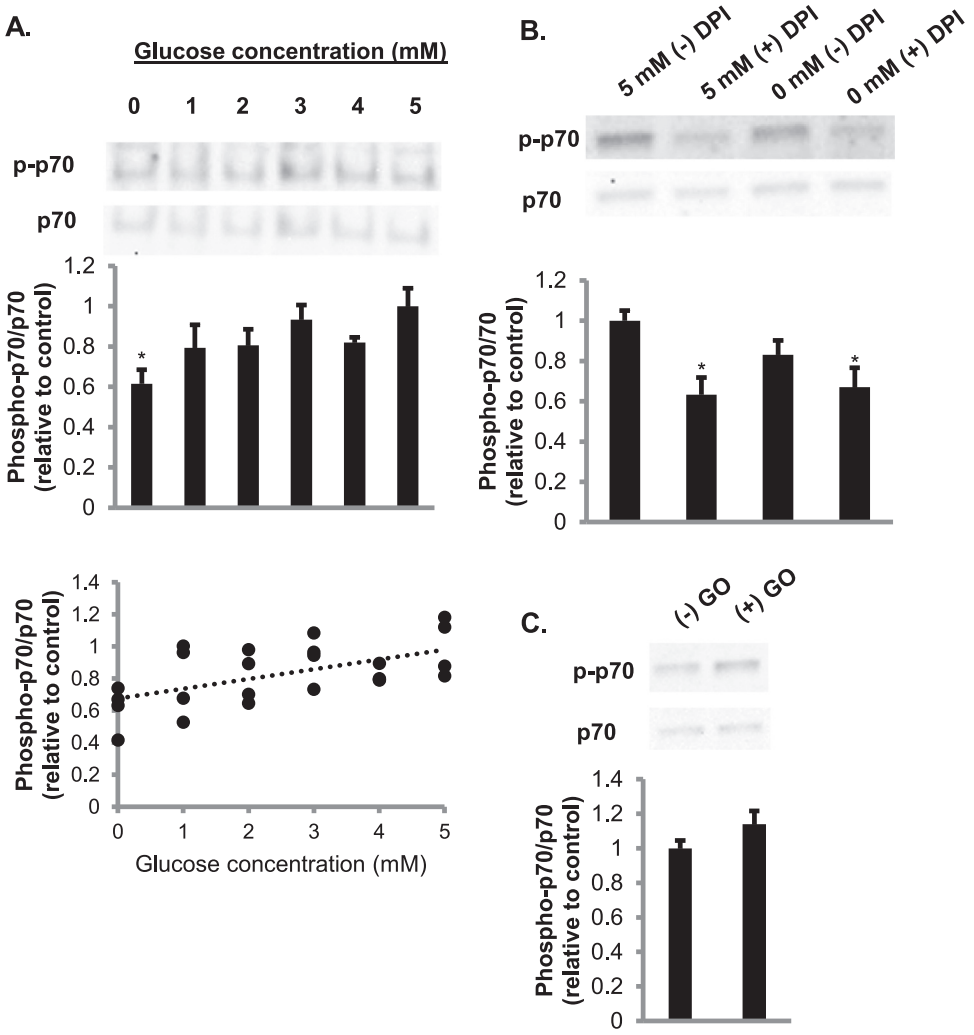

Fig. 8. Glucose-dependent phosphorylation of $p70^{S6k}$ requires NOX enzymes. A. Cells incubated with increasing concentrations of glucose were utilized in western blot analysis of the phosphorylation of $p70^{S6k}$ (N = 4/group). Error bars represent standard error of the mean. ANOVA was performed *p < 0.05 vs 5 mM glucose. Correlation analysis is shown by the scatterplot (r = 0.57, p = 0.004). **B.** Cells pretreated in 0 or 5 mM glucose as well as in the presence or absence of 20 μM DPI were used for western blot analysis of the phosphorylation of $p70^{S6k}$ (N = 6/group). Error bars represent standard error of the mean. ANOVA was performed *p < 0.05 vs 5 mM glucose (-) DPI **C.** Cells incubated in the presence or absence of 50 mU/mL glucose oxidase were analyzed by western blot analysis of the phosphorylation of $p70^{S6k}$. (N = 6/group). Error bars represent standard error of the mean. ANOVA was performed.

4. Discussion

Previous literature has demonstrated that skeletal muscle is capable of tPMET [11], but novel information provided by this study shows that the production of superoxide through tPMET is dependent on presence of extracellular glucose. Further, this glucose-sensitive process occurs through the PPP, rather than glycolysis. In this process, NADPH produced through the PPP is utilized by NOX1 to generate superoxide. Importantly, this study has also demonstrated glucose- and NOX-dependent phosphorylation of $p70^{S6k}$ in the absence of changes in AKT phosphorylation, suggesting a novel mechanism for cellular glucose sensing.

Previous research has established glucose as a physiological signal that is sensed in multiple tissues [26]. Pancreatic beta cells (β-cells), neurons, and hepatocytes are three cells types that have mechanisms of glucose sensing dependent on GLUT2-mediated glucose uptake followed by glucose phosphorylation [27–29]. For example, pancreatic β-cells have a well-established mechanism for glucose sensing with a primary role in regulation of insulin secretion [30]. Glucose is taken up into the cell through GLUT2, providing substrate for generation of ATP. This leads to inactivation of ATP-sensitive potassium channels and subsequent insulin secretion. Recently, an alternative pathway of insulin secretion has been elucidated in β-cells. In this new mechanism, intermediates from the TCA cycle are utilized to produce reduced glutathione [31]. Glutathione reduces glutaredoxin, activating sentrin/SUMO-specific protease-1 (SENP-1) release of insulin. This production of glutathione may rely on mitochondrial generation of NADPH by isocitrate dehydrogenase. Notably, the current study implicates PPP-derived NADPH, as opposed to NADPH from mitochondrially-produced substrates, in glucose-sensing.

Glucose sensing can differ in neurons, which are found throughout the hypothalamus, where glucose can either activate neurons in high or low glucose concentrations [32]. Glucose sensing in which neurons increase their firing rate in high glucose conditions is similar to that found in β-cells due to the same isoform of glucokinase located in the hypothalamus as well as co-localization of GLUT2 and glucokinase [27,33]. When glucose concentrations are low, this can increase neuron firing by activating AMP-activated protein kinase (AMPK) which could then suppress cystic fibrosis trans-membrane regulator and affect the depolarization of the membrane [32]. In the current study, AMPK phosphorylation did not vary as glucose concentration increased from 1 mM to 5 mM (data not shown), suggesting that the glucose-sensing described in the current study leading to $P70^{S6k}$ phosphorylation does not involve AMPK.

While hepatocytes have been shown to be capable of glucose sensing, GLUT2 is not a contributing factor. Glucokinase is still a significant contributor to this process in conjunction with carbohydrate responsive element-binding protein (ChREBP), a transcription factor that is sensitive to glucose [34]. When glucokinase was knocked down, there was a significant suppression in ChREBP mRNA and ChREBP expression was no longer stimulated at high concentrations of glucose. There was also a notable decrease in levels of xylulose 5-phosphate,

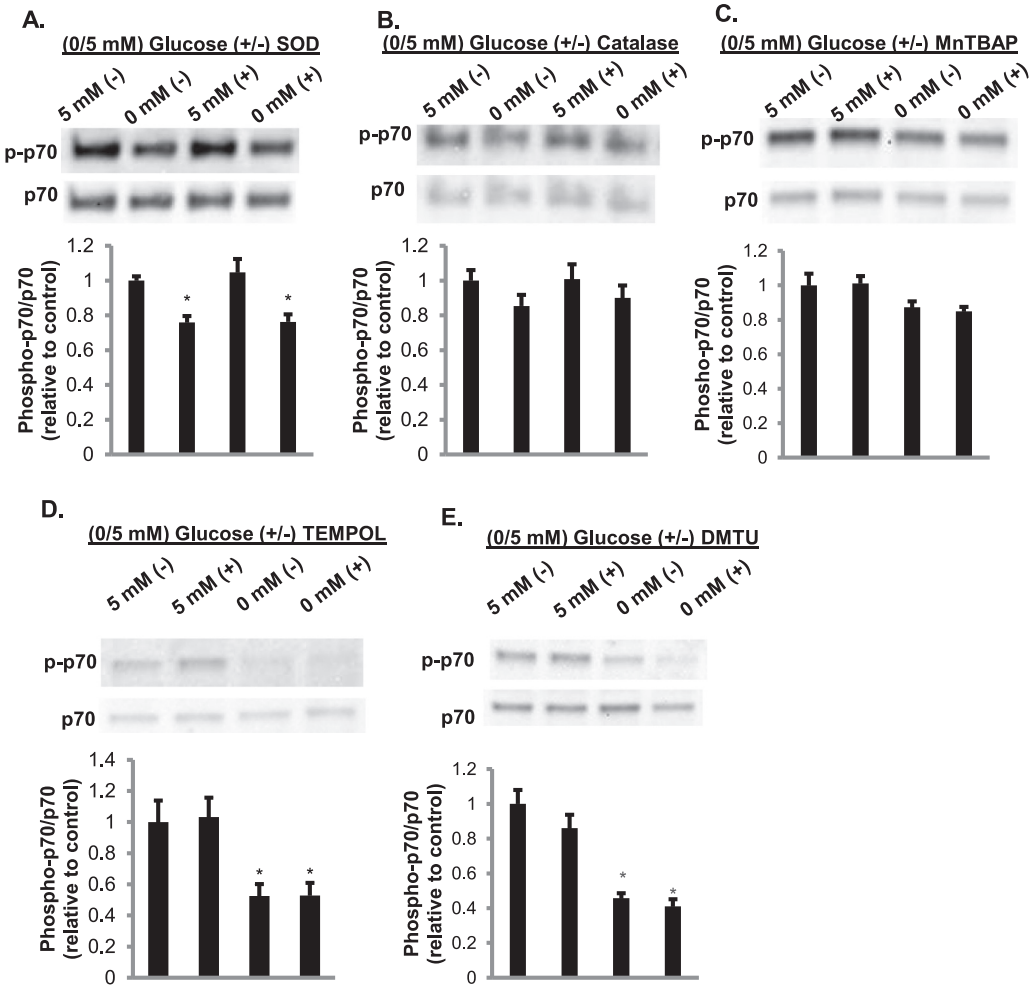

Fig. 9. Extracellular superoxide and peroxide and intracellular superoxide do not play a role in phosphorylation of p70^{S6k}. Cells treated with and without 60 U/mL SOD (**A**), 100 U/mL catalase (**B**), 150 μM MnTBAP (**C**), 1 mM TEMPOL (**D**), or 5 mM DMTU (**E**), were analyzed for phosphorylated p70^{S6k}. Total p70 was utilized as a loading control and used to quantify the western (N = 3/group). Error bars represent standard error of the mean. ANOVA was performed *p < 0.05 vs 5 mM glucose (-) enzyme.

which is a product of the PPP and has been shown to activate ChREBP. These findings suggest that glucose sensing in hepatocytes is dependent on generation of xylulose 5-phosphate by the PPP [29,34]. The current study suggests that the PPP plays a role in glucose sensing by production of NADPH as opposed to the xylulose 5-phosphate that might underlie hepatocyte glucose sensing.

NADPH oxidases have been implicated in the glucose-sensing process in β-cells. Components of NOX enzymes have been isolated from

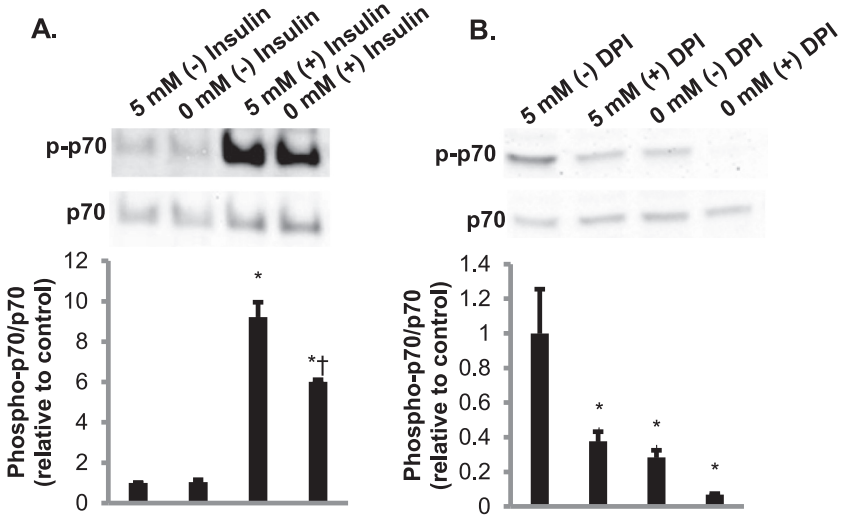

Fig. 10. Insulin-stimulated phosphorylation of p70^{S6k} is dependent on glucose and NOX. A. Cells treated with 2 mM pyruvate or 5 mM glucose with and without 5 nM insulin were analyzed for phosphorylated p70^{S6k}. Total p70 was utilized as a loading control and used to quantity the western (N = 3/group). Error bars represent standard error of the mean. ANOVA was performed *p < 0.05 vs 5 mM glucose (-) insulin †p < 0.05 vs 5 mM glucose (+) insulin. **B.** Cells treated with 2 mM pyruvate or 5 mM glucose with 5 nM insulin in the presence or absence of 20 μM DPI were analyzed for phosphorylated p70^{S6k}. Total p70 was utilized as a loading control and used to quantity the western (N = 3/group). Error bars represent standard error of the mean. ANOVA was performed *p < 0.05 vs 5 mM glucose (-) DPI.

the cytosol of β-cells and NOX1, 2 and 4 isoforms have been detected in β-cell membranes [35]. When NOX enzymes in pancreatic islets cells were inhibited with DPI, there was a decrease in insulin secretion at higher levels of glucose [36]. There was also suppression of GLUT2 and glucokinase expression after treatment with DPI. Due to this suppression of glucose-stimulated insulin increase and GLUT2 and glucokinase gene expression, it seems likely that NOX enzymes play a role in the glucose-sensing mechanism in β-cells.

The insulin signaling pathway, MAPK pathway, $p70^{S6k}$ pathway, and calcium channels have all been shown to be activated by ROS [22–24,37]. For example, in vascular smooth muscle cells, the addition of H_2O_2 significantly suppressed AKT activation and this activation was inhibited by catalase [37]. AKT phosphorylation, as well as insulin receptor tyrosyl phosphorylation, was also shown to be reduced by NOX4 knockdown in 3T3-L1 adipocytes [38]. Similar increases in phosphorylation of AKT were also seen in HepG2 cells that produce superoxide upon stimulation with NADH [39]. This phosphorylation was inhibited after the addition of catalase and NAC. Taken together, these findings suggest that H_2O_2 can activate the insulin signaling pathway. While it is beyond the scope of this study to determine why the insulin signaling pathway, the MAPK pathway, and calcium channels were not responsive to glucose in the same way as $p70^{S6k}$ phosphorylation, we speculate that this is dependent on both the localization and the abundance of the ROS signal, as has been proposed for differential responses to ROS in models of aging [40].

The serine/threonine kinase $p70^{S6k}$ is involved in many cellular functions including protein synthesis, cell growth and cell cycle progression, cell migration, cell survival, and regulation of insulin signaling [41–45]. One of the primary roles of $p70^{S6k}$ is to phosphorylate the 40 S ribosomal protein S6, and therefore, one of the leading functions of $p70^{S6k}$ is to stimulate protein synthesis [41]. This has been demonstrated through a dominant-interfering $p70^{S6k}$ mutant that prevented the activation of $p70^{S6k}$ as well as the translation of the 5′ terminal oligopyrimidine tract mRNA, which aids in translational regulation [41]. This indicates that $p70^{S6k}$ plays a direct role in translational control and protein synthesis. Our data suggest a novel glucose-sensing pathway linking nutrient availability to impact on the $p70^{S6k}$ pathway.

In summary, we have demonstrated a glucose-sensing role of tPMET in skeletal muscle cells that is dependent upon the pentose phosphate pathway and NOX1. In addition, we have uncovered a novel NOX-dependent glucose sensing pathway for selective phosphorylation of $p70^{S6k}$ without affecting AKT or MAPK. Further, insulin-stimulated phosphorylation of $p70^{S6k}$ was dependent on both glucose and NOX. These findings suggest that muscle cells have a novel NOX-dependent pathway linking glucose-sensing to selective regulation of $p70^{S6k}$, a key player in cell growth and proliferation.

Acknowledgements

The authors would like to thank Thomas Bell and Lyn Mattathil for their technical assistance.

Grants

This work was supported by United States Public Health Service award R15DK102122 from the National Institute of Diabetes and Digestive and Kidney Diseases (NIDDK) to Jonathan Fisher. The manuscript content is solely the responsibility of the authors and does not necessarily represent the official views of the NIDDK or the National Institutes of Health.

Author contributions

Shannon C. Kelly (SCK), Neej N. Patel, and Amanda M. Eccardt played roles in conceptualization, formal analysis, investigation, methodology, and writing (review and editing). Jonathan S. Fisher (JSF) had roles in conceptualization, formal analysis, methology, funding acquisition, supervision, and writing (review and editing). SCK wrote the original draft with review and editing by JSF. SCK also had a role in review and editing.

Disclosures

The authors declare no conflict of interest.

References

[1] F.L. Crane, I.L. Sun, M.G. Clark, C. Grenbing, H. Low, Transplasma-membrane redox systems in growth and development, Biochim. Biophys. Acta 811 (1985) 233–264.
[2] E. Lesuisse, F. Raguzzi, R.R. Crichton, Iron uptake by the yeast Saccharomyces cerevisiae: involvement of a reduction step, J. Gen. Microbiol. 133 (1987) 3229–3236.
[3] A. del Castillo-Olivares, A. Esteban del Valle, J. Marquez, I. Nunez de Castro, M.A. Medina, Ehrlich cell plasma membrane redox system is modulated through signal transduction pathways involving cGMP and Ca2+ as second messengers, J. Bioenerg. Biomembr. 27 (1995) 605–611.
[4] C. Diaz-Gomez, J.M. Villalba, R. Perez-Vicente, F. Crane, Ascorbate stabilization Is stimulated in rho(0)HL-60 cells by CoQ10 increase at the plasma membrane, Biochem. Biophys. Res. Commun. 234 (1997) 79–81.
[5] S. Furukawa, T. Fujita, M. Shimabukuro, M. Iwaki, Y. Yamada, Y. Nakajima, O. Nakayama, M. Makishima, M. Matsuda, I. Shimomura, Increased oxidative stress in obesity and its impact on metabolic syndrome, J. Clin. Investig. 114 (2004) 1752–1761.
[6] A. Baoutina, R.T. Dean, W. Jessup, Trans-plasma membrane electron transport induces macrophage-mediated low density lipoprotein oxidation, FASEB J. 15 (2001) 1580–1582.
[7] M.A. Medina, A. del Castillo-Olivares, L. Schweigerer, Plasma membrane redox activity correlates with N-myc expression in neuroblastoma cells, FEBS Lett. 311 (1992) 99–101.
[8] A.J. Bruce-Keller, S. Gupta, T.E. Parrino, A.G. Knight, P.J. Ebenezer, A.M. Weidner, H. LeVine, J.N. Keller, W.R. Markesbery, NOX activity is increased in mild cognitive impairment, Antioxid. Redox Signal 12 (2010) 1371–1382.
[9] L. Hecker, R. Vittal, T. Jones, R. Jagirdar, T.R. Luckhardt, J.C. Horowitz, S. Pennathur, F.J. Martinez, V.J. Thannickal, NADPH oxidase-4 mediates myofibroblast activation and fibrogenic responses to lung injury, Nat. Med. 15 (2009) 1077–1081.
[10] D. Del Principe, L. Avigliano, I. Savini, M.V. Catani, Trans-plasma membrane electron transport in mammals: functional significance in health and disease, Antioxid. Redox Signal 14 (2011) 2289–2318.
[11] A.M. Eccardt, T.P. Bell, L. Mattathil, R.M. Prasad, S.C. Kelly, J.S. Fisher, Trans-plasma membrane electron transport and ascorbate efflux by skeletal muscle, Antioxidants 6 (2017) 89.
[12] S.C. Kelly, A.M. Eccardt, J.S. Fisher, Measuring trans-plasma membrane electron transport by C2C12 myotubes, J. Vis. Exp. 135 (2018) e57565.
[13] L.D. Spears, A.V. Tran, C.Y. Qin, S.B. Hobbs, C.A. Burns, N.K. Royer, Z. Zhang, L. Ralston, J.S. Fisher, Chloroquine increases phosphorylation of AMPK and Akt in myotubes, Heliyon 2 (2016) e00083.
[14] S. Andrisse, G.D. Patel, J.E. Chen, A.M. Webber, L.D. Spears, R.M. Koehler, R.M. Robinson-Hill, J.K. Ching, I. Jeong, J.S. Fisher, ATM and GLUT1-S490phosphorylation regulate GLUT1 mediated transport in skeletal muscle, PLoS One 8 (2013) e66027.
[15] H. Wang, Z. Li, R. Yumul, S. Lara, A. Hemminki, P. Fender, A. Lieber, Multimerization of adenovirus serotype 3 fiber knob domains is required for efficient binding of virus to desmoglein 2 and subsequent opening of epithelial junctions, J. Virol. 85 (2011) 6390–6402.
[16] M. Sagi, R. Fluhr, Superoxide production by plant homologues of the gp91(phox) NADPH oxidase. Modulation of activity by calcium and by tobacco mosaic virus infection, Plant Physiol. 126 (2001) 1281–1290.
[17] K. Lin, W. Sadee, J. Quillan, Rapid measurements of intracellular calcium using a fluorescent plate reader, Biotechniques 26 (1999) 318–322.
[18] Y.J. Piao, Y.H. Seo, F. Hong, J.H. Kim, Y. Kim, M.H. Kang, B.S. Kim, S.A. Jo, I. Jo, D. Jue, I. Kang, J. Ha, S.S. Kim, Nox 2 stimulates muscle differentiation via NF-nB/iNOS pathway, Free Radic. Biol. Med. 38 (2005) 989–1001.
[19] S. Altenhofer, K.A. Radermacher, P.W. Kleikers, K. Wingler, H.H. Schmidt, Evolution of NADPH oxidase inhibitors: selectivity and mechanisms for target engagement, Antioxid. Redox Signal 23 (2015) 406–427.
[20] M. Di Monaco, A. Pizzini, V. Gatto, L. Leonardi, M. Gallo, E. Brignardello, G. Boccuzzi, Role of glucose-6-phosphate dehydrogenase inhibition in the antiproliferative effects of dehydroepiandrosterone on human breast cancer cells, Br. J. Cancer 75 (1997) 589–592.
[21] C. Granchi, F. Minutolo, Anti-cancer agents that counteract tumor glycolysis, Chem. Med Chem. 7 (2012) 1318–1350.
[22] M. Ushio-Fukai, R. Alexander, M. Akers, K. Griendling, p38 mitogen-activated protein kinase is a critical component of the redox-sensitive signaling pathways activated by angiotensin II, J. Biol. Chem. 273 (1998) 15022–15029.
[23] M.C. Zimmerman, R.V. Sharma, R.L. Davisson, Superoxide mediates angiotensin II-induced influx of extracellular calcium in neural cells, Hypertension 45 (2005)

717–723.
[24] C. Huang, J. Li, Q. Ke, S. Leonard, B. Jiang, X. Zhong, M. Costa, V. Castranova, X. Shi, Ultraviolet-induced phosphorylation ofp70(S6K) at Thr(389) and Thr(421)/Ser(424) involves hydrogen peroxide and mammalian target of rapamycin but not Akt and atypical protein kinase C, Cancer Res. 62 (2002) 5689–5697.
[25] J.C. Jagtap, A. Chandele, B.A. Chopde, P. Shastry, Sodium pyruvate protects against H2O2 mediated apoptosis in human neuroblastoma cell line-SK-N-MC, J. Chem. Neuroanat. 26 (2003) 109–118.
[26] B. Thorens, Glucose sensing and the pathogenesis of obesity and type 2 diabetes, Int. J. Obes. 32 (Suppl 6) (2005) S62–S71 (2008).
[27] F.C. Schuit, P. Huypens, H. Heimberg, D.G. Pipeleers, Glucose sensing in pancreatic beta-cells: a model for the study of other glucose-regulated cells in gut, pancreas, and hypothalamus, Diabetes 50 (2001) 1–11.
[28] F. Matschinsky, B. Glaser, M. Magnuson, Pancreatic beta-cell glucokinase: closing the gap between theoretical concepts and experimental realities, Diabetes 47 (1998) 307–315.
[29] M.H. Oosterveer, K. Schoonjans, Hepatic glucose sensing and integrative pathways in the liver, Cell Mol. Life Sci. 71 (2014) 1453–1467.
[30] P.E. MacDonald, J.W. Joseph, P. Rorsman, Glucose-sensing mechanisms in pancreatic beta-cells, Philos. Trans. R. Soc. Lond. B Biol. Sci. 360 (2005) 2211–2225.
[31] M.V. Jensen, J.R. Gooding, M. Ferdaoussi, X.Q. Dai, B.S. Peterson, P.E. MacDonald, C.B. Newgard, Metabolomics applied to islet nutrient sensing mechanisms, Diabetes Obes. Metab. 19 (Suppl. 1) (2017) S90–S94.
[32] L. Steinbusch, G. Labouebe, B. Thorens, Brain glucose sensing in homeostatic and hedonic regulation, Trends Endocrinol. Metab. 26 (2015) 455–466.
[33] M. Navarro, F. Rodriguez de Fonseca, E. Alvarez, J. Chowen, J. Zueco, R. Gomez, J. Eng, E. Blazquez, Colocalization of glucagon-like peptide-1 (GLP-1) receptors, glucose transporter GLUT-2, and glucokinase mRNAs in rat hypothalamic cells: evidence for a role of GLP-1 receptor agonists as an inhibitory signal for food and water intake, J. Neurochem. 67 (1996) 1982–1991.
[34] R. Dentin, J.P. Pegorier, F. Benhamed, F. Foufelle, P. Ferre, V. Fauveau, M.A. Magnuson, J. Girard, C. Postic, Hepatic glucokinase is required for the synergistic action of ChREBP and SREBP-1c on glycolytic and lipogenic gene expression, J. Biol. Chem. 279 (2004) 20314–20326.
[35] Y. Uchizono, Takeya, R. Iwase, M. Sasaki, N. Oku, M. Imoto, H. Iida, M. Sumimoto, H. Expression, of isoforms of NADPH oxidase components in rat pancreatic islets, Life Sci. 80 (2006) 133–139.
[36] D. Morgan, E. Rebelato, F. Abdulkader, M.F. Graciano, H.R. Oliveira-Emilio, A.E. Hirata, M.S. Rocha, S. Bordin, R. Curi, A.R. Carpinelli, Association of NAD(P)H oxidase with glucose-induced insulin secretion by pancreatic beta-cells, Endocrinology 150 (2009) 2197–2201.
[37] M. Ushio-Fukai, R.W. Alexander, M. Akers, Q. Yin, Y. Fujio, K. Walsh, K.K. Griendling, Reactive oxygen species mediate the activation of Akt/protein kinase B by angiotensin II in vascular smooth muscle cells, J. Biol. Chem. 274 (1999) 22699–22704.
[38] K. Mahadev, H. Motoshima, X. Wu, J.M. Ruddy, R.S. Arnold, G. Cheng, J.D. Lambeth, B.J. Goldstein, The NAD(P)H oxidase homolog Nox4 modulates insulin-stimulated generation of H2O2 and plays an integral role in insulin signal transduction, Mol. Cell Biol. 24 (2004) 1844–1854.
[39] H. Lee, B.W. Kim, J.W. Lee, J. Hong, J.W. Lee, H.L. Kim, J.S. Lee, Y.G. Ko, Extracellular reactive oxygen species are generated by a plasma membrane oxidative phosphorylation system, Free Radic. Biol. Med. 112 (2017) 504–514.
[40] J.M. Van Raamsdonk, Levels and location are crucial in determining the effect of ROS on lifespan, Worm 4 (2015) e1094607.
[41] H. Jefferies, Fumagalli, S. Dennis, P. Reinhard, C. Pearson, R. Thomas, G. Rapamycin, suppresses 5'TOP mRNA translation through inhibition of p70s6k, EMBO J. 16 (1997) 3693–3704.
[42] H. Shima, M. Pende, Y. Chen, S. Fumagalli, G. Thomas, S. Kozma, Disruption of thep70(s6k)/p85(s6k) gene reveals a small mouse phenotype and a new functional S6 kinase, EMBO J. 17 (1998) 6649–6659.
[43] J. Chung, C.J. Kuo, G.R. Crabtree, J. Blenis, Rapamycin-FKBP specifically blocks growth-dependent activation of and signaling by the 70 kd S6 protein kinases, Cell 69 (1992) 1227–1236.
[44] H. Harada, J. Andersen, M. Mann, N. Terada, S. Korsmeyer, p70S6 kinase signals cell survival as well as growth, inactivating the pro-apoptotic molecule BAD, Proc. Natl. Acad. Sci. USA 98 (2001) 9666–9670.
[45] T. Haruta, T. Uno, J. Kawahara, A. Takano, K. Egawa, P.M. Sharma, J.M. Olefsky, M. Kobayashi, A rapamycin-sensitive pathway down-regulates insulin signaling via phosphorylation and proteasomal degradation of insulin receptor substrate-1, Mol. Endocrinol. 14 (2000) 783–794.